STEREO IMPACT

PROBLEM REPORT
PR-1029
FM1 SWEA Anode 2
2004-12-20

PR Numbers: 1xxx=UCB, 2xxx=Caltech/JPL, 3xxx=UMd, 4xxx=GSFC/SEP, 5xxx=GSFC/Mag, 6xxx=CESR, 7xxx=Keil, 8xxx=ESTEC, 9xxx=MPAe

Assembly : SWEA/STE-D	**SubAssembly :**
Component/Part Number:	**Serial Number:** FM1
Originator: David Curtis	**Organization:** U.C. Berkeley
Phone : 510-642-5998	**Email :** dwc@ssl.berkeley.edu

Failure Occurred During (Check one √)

√ Functional test □ Qualification test □ S/C Integration □ Launch operations

Environment when failure occurred:

□ Ambient □ Vibration □ Shock □ Acoustic
□ Thermal √ Vacuum □ Thermal-Vacuum □ EMI/EMC

Problem Description

During SWEA FM1 Calibrations it was discovered that Anode number 2 stopped counting after the instrument had been on for several hours. It would return to functionality after being turned off for a while. Both real counts from the MCP and counts from the test pulser are missing.

Analyses Performed to Determine Cause

It was found that the counts drop-out were correlated with the temperature of the instrument. The problem occurs above +40C, which is right at the top of the operational range, and well above the on-orbit predicts. The unit was disassembled and subsystems were tested individually in a thermal chamber. The problem was localized to the SWEA detector, (as opposed to the Actel that contains the counter, or the harness in between). Observing the SWEA output with an oscilloscope in this configuration when above +40C shows that the Anode 2 preamp/discriminator output changes from the normal pulse to a small glitch.

Corrective Action/ Resolution

□ Rework √ Repair □ Use As Is □ Scrap

Replace the Amptek A111F preamp for Anode #2 (see schematic below). Test at up to +50C, with no dropout. Send failed preamp to failure analysis. Part removed LDC 0048, serial number 206. New part same LDC, serial number 240.

Failure analysis attached (Q50006 and Q50370). Poor workmanship (bonding) found to be the root cause. Accelerated life testing of spare flight lot parts show low probability of further on-orbit failure. No found problems during instrument environmental tests enhance reliability. Instrument can meet minimum science requirements with half of the 16 preamps failed. Plan is to fly as-is, but build and test a backup preamp board (with preamps from a new lot) in case of problems late in the test flow (done).

Date Action Taken: 2004-12-22 **Retest Results**: Success

Corrective Action Required/Performed on other Units □ Serial Number(s): _____

Closure Approvals

Subsystem Lead: _____ Date:_____
IMPACT Project Manager: _____ Date _____
IMPACT QA: _____ Date:_____
NASA IMPACT Instrument Manager: _____ Date:_____

SWEA Amplifier board. Failed/replaced part is U3.

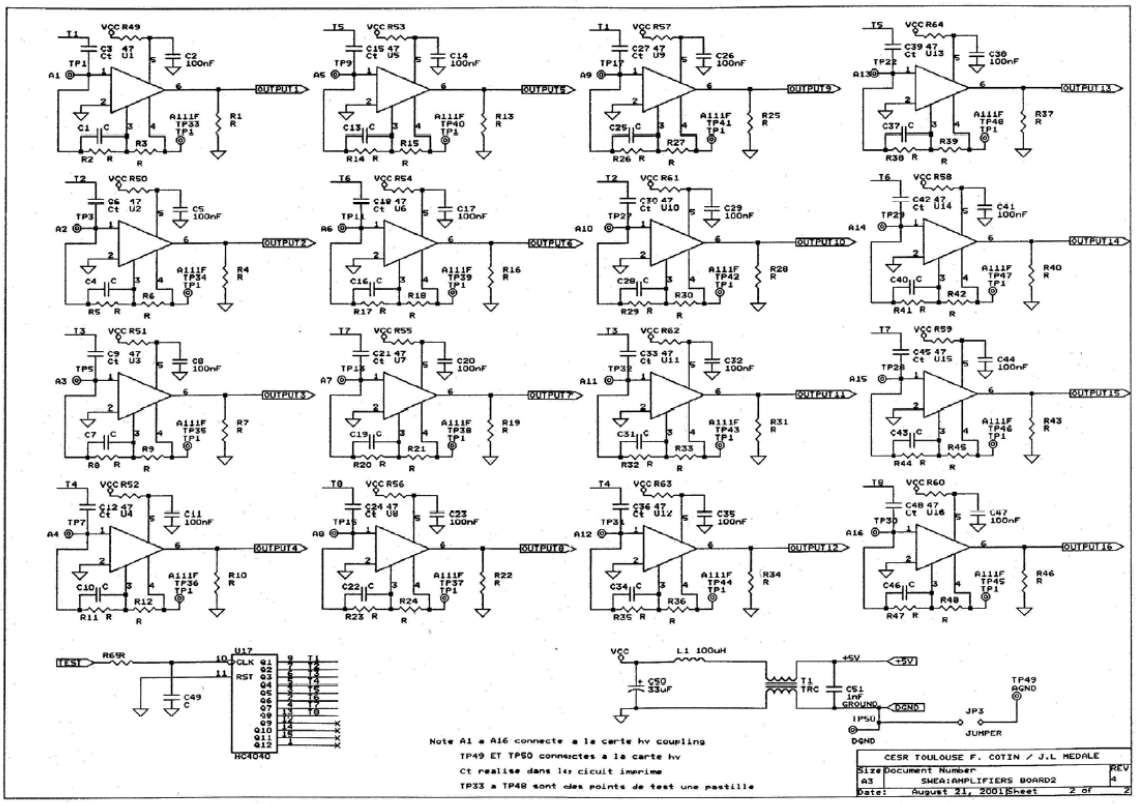

T3 is the test pulser input, 5V square wave.
A3 connects to the anode which collects the MCP signal.
Ct is ~0.3pF, built into the PWB
R7, R8, R9 are not loaded.

GODDARD SPACE FLIGHT CENTER

Failure Analysis Report

Charge Sensitive Pre-Amp & Discriminator Hybrid
Mfr.: Amptek, Inc.
P/N: A111F
DC: 0048
SN: 206

Project
STEREO
System
IMPACT-SWEA/STE-D
Requester
A. Reyes (562)
Report Date
03/03/2005

Investigator
C. Greenwell (562)
M. McClendon (541)

Background

The output of the Amptek A111F pre-amp/discriminator hybrid was documented to fail after the system it was in was powered up for several hours. The output was functional after the system was powered off for a while. Additional testing revealed the malfunction was correlated to operating temperatures above +40C.

Part Description

The Amptek A111F is a charge sensitive preamplifier, discriminator and pulse shaper developed especially for instrumentation employing microchannel plates (MCP) and other low capacitance charge producing detectors.

The device is built using standard hybrid microelectronic construction. A single sided ceramic substrate with laser-trimmed thick film resistors has several diodes, transistors, capacitors and a surface mount resistor, mounted to it with conductive and non-conductive epoxies. The discrete devices are interconnected with 1.25-mil gold bond wires. The device is provided in a hermetic, 6-pin, single in-line, metal package.

Analysis and Discussion

External and radiographic inspections revealed no anomalies. Figures 1 and 2 show external and radiographic images of the device. The device passed fine and gross hermeticity testing and also PIND testing.

Pin to pin curve tracer testing revealed no obvious anomaly, however, a “known good devices” was not available for comparison. Curve tracing was performed at ambient room temperature and at 45° with no differences observed (except for diode voltage shifts consistent with the change in test temperature).

Functional testing was performed using a test fixture and procedures provided by Amptek. The device passed the first two tests, supply current and threshold, both at 5 volts, but then failed at test three when the voltage was increased to 10 volts. Power supply current increased from 1.18mA (spec – 1.3 +/- 0.2 mA) to over 12 mA and the output dropped out. The device did not recover after power cycling and after several hours with power off. Curve tracer testing was repeated and there was no change in any pin-to-pin combination.

Internal examination revealed interconnect wire ball bonds at one of the transistors were placed such that they touched (and shorted to) the unpassivated die edge. It was noted that the ball bonds at this transistor and other locations within the assembly were quite large in diameter compared to the wire diameter. Some appeared to be larger than 5 wire diameters, which is unacceptable in MIL-STD-750 and 883.

The transistor in question was a dual transistor pair on a single die (of which there are three such dice within the hybrid). For the purpose of this investigation the transistors were designated Q9 and Q10. The emitter ball bonds for both Q9 and Q10 appeared to be touching the unpassivated die edge, while the Q10 base bond appeared extremely close to touching. A study of the circuit layout showed the Q10 collector directly drives the base of the output transistor. Figures 3 shows an overall internal view of the hybrid with the suspected shorted transistor identified. Figure 4 shows a closer view of the Q9/Q10 transistor and local area. Figures 5 and 6 show optical images of the misplaced ball bonds at Q9 and Q10

SEM inspection further documented the poorly placed ball bonds, as seen in Figures 7 through 10, and showed that the ball bonds, including the Q10 base (Q10-B) ball bond, was indeed touching the unpassivated die edge. While inspecting in the SEM, EDS was used to confirm the unpassivated die edge. The unpassivated die edge is a very common feature on microelectronic dice.

The Q9/Q10 transistors were isolated from the circuit by removing the bond wires (all six of which exhibited excellent pull strengths). Micro-probing the die revealed a 687-ohm short between Q10 emitter and base. Q9 emitter-base diode displayed nominal forward and reverse characteristics. Q9-E, Q10-E and Q10-B displayed nonlinear characteristics to ground (through the bulk/backside of the die).

Next, the Q9/Q10 transistor die was removed from the package. The transistors were again characterized and no change was noted. The ball remnant at Q10-B was removed and final micro-probing revealed the emitter-base short was now gone. The Q10 emitter-base diode was again compared to the Q9 emitter-base diode and both were nearly identical. Curve tracer plots for these results are shown in Figures 11 and 12.

A non-related but nonetheless very serious defect was found on the Q9/Q10 transistor die. The aluminum metallization suffered severe step coverage reduction at oxide steps on the die surface. It appeared that the metallization was nearly open circuit. Figures 13 and 14 show this condition.

Conclusion

The failure of the A111F device was confirmed. The cause of failure was a workmanship error that resulted in relatively large diameter ball bonds shorting to the unpassivated die edge of the transistor that drives the output stage of the hybrid. A thorough quality control inspection at the manufacturer should have revealed this workmanship defect. A pre-cap customer source inspection (CSI) also could be expected to reveal such a defect.

The secondary finding of unacceptable metallization on the Q9/Q10 transistor is also of serious concern. Optical inspections would not reveal this defect, but a destructive physical analysis (DPA) is expected to find this type defect.

As is, these device would not be recommended for space flight use. It is recommended that the lot date code for all A111F devices used on the STEREO-IMPACT/SWEA instrument be identified and several pieces of each date code be submitted for DPA. Replacing these device may be necessary.

NASA GODDARD SPACE FLIGHT CENTER

Part Type:	Hybrid	Part No:	A111F
Manufacturer:	Amptek	Date Code:	0048

Appended Images:

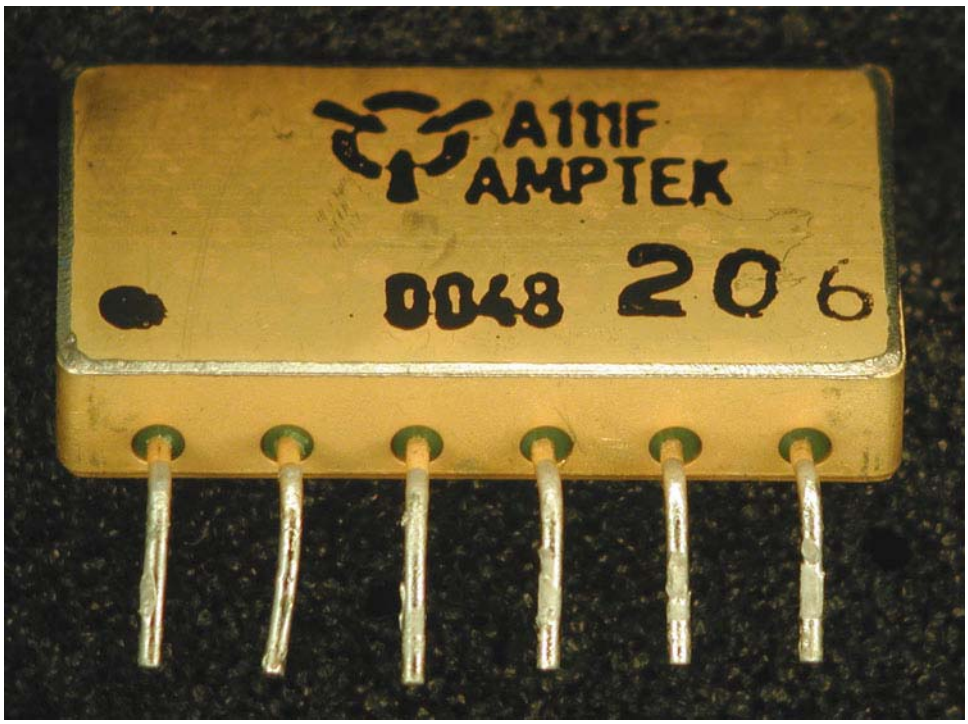

Figure 1. External view of the A111F device.

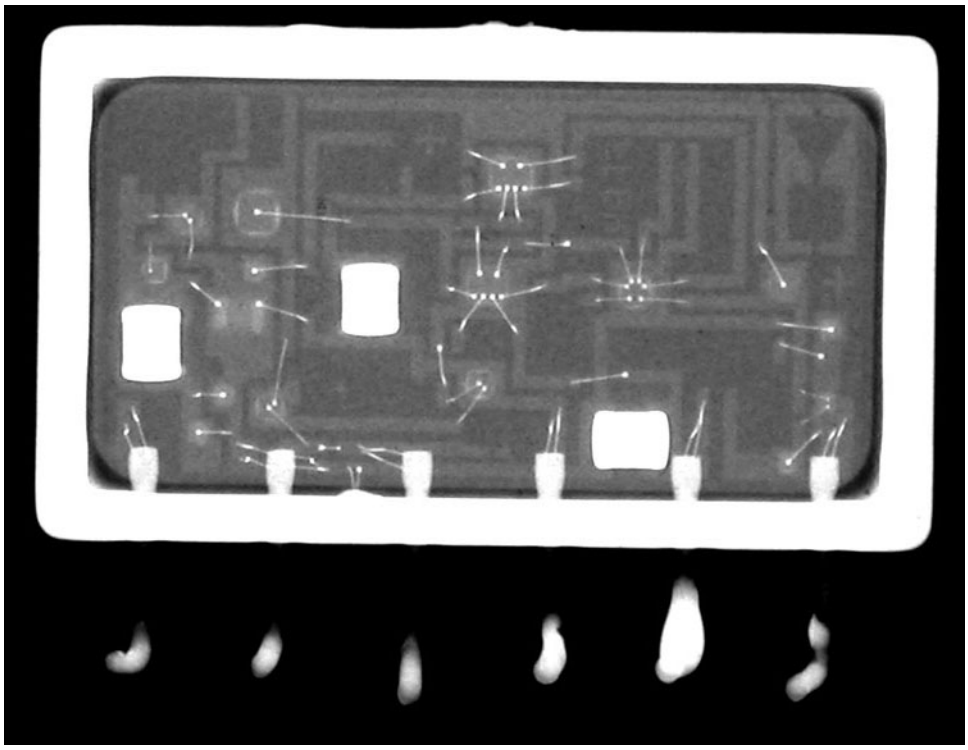

Figure 2. Radiographic view of the device.

Part Type: Hybrid Part No: A111F
Manufacturer: Amptek Date Code: 0048

Appended Images:

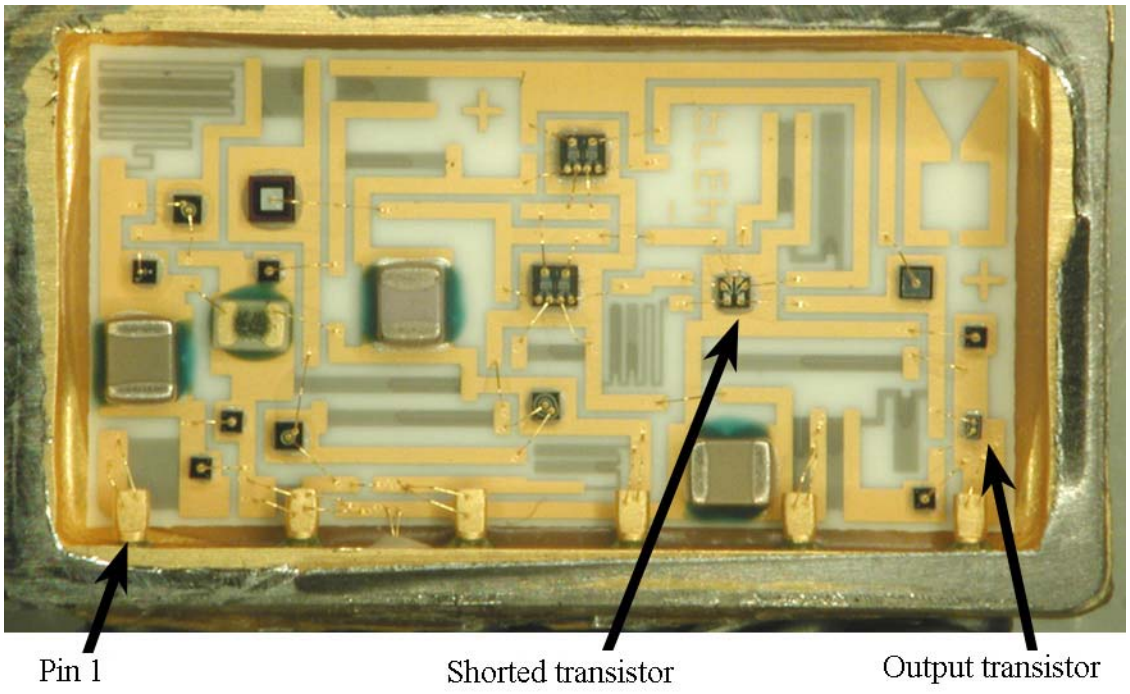

Figure 3. Overall internal cavity view of the failed A111F charge amplifier.

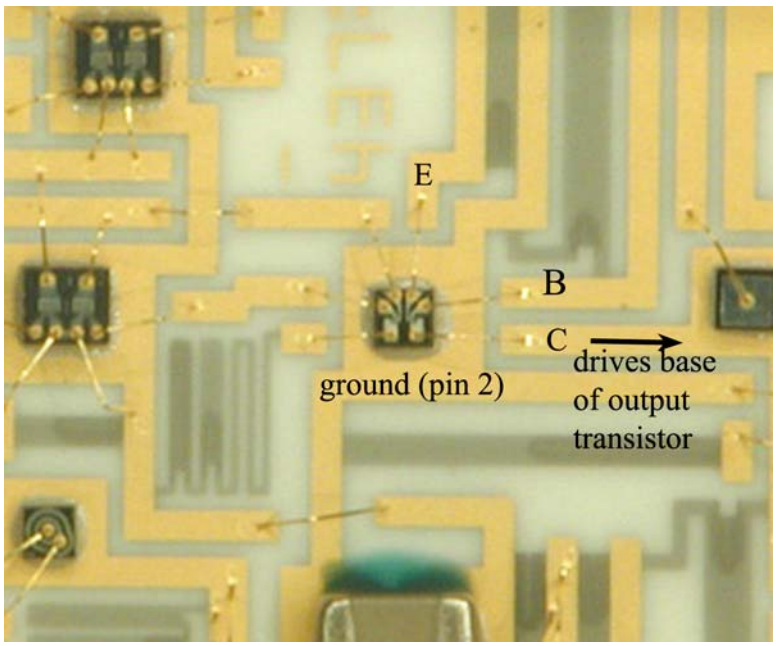

Figure 4. Close-up of area of the shorted transistor. The transistor is mounted directly to pin 2 ground metal. The collector of the shorted transistor directly drives the base of the output transistor.

NASA GODDARD SPACE FLIGHT CENTER

Part Type:	Hybrid	Part No:	A111F
Manufacturer:	Amptek	Date Code:	0048

Appended Images:

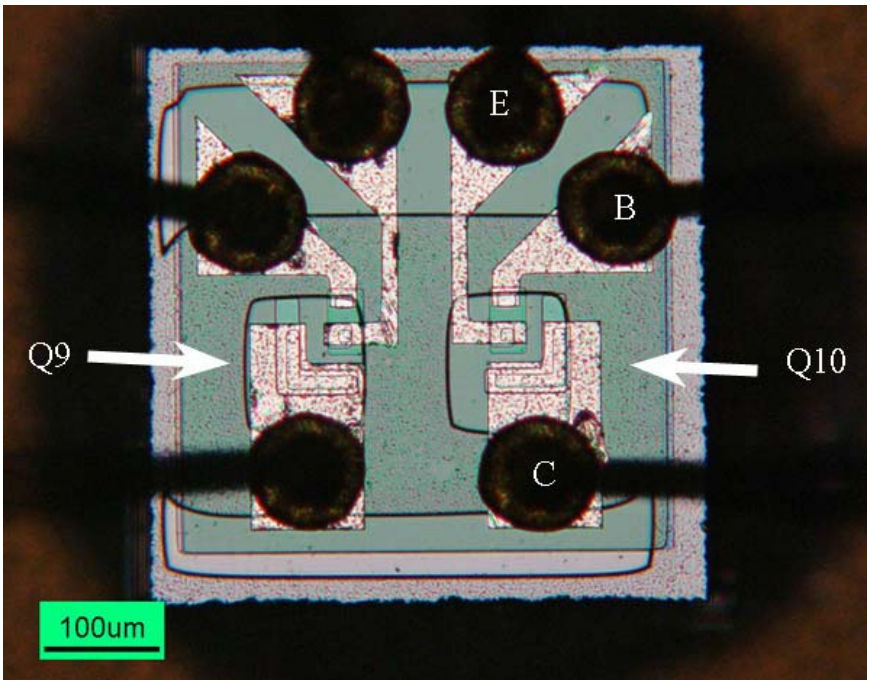

Figure 5. Optical image of shorted transistor die.

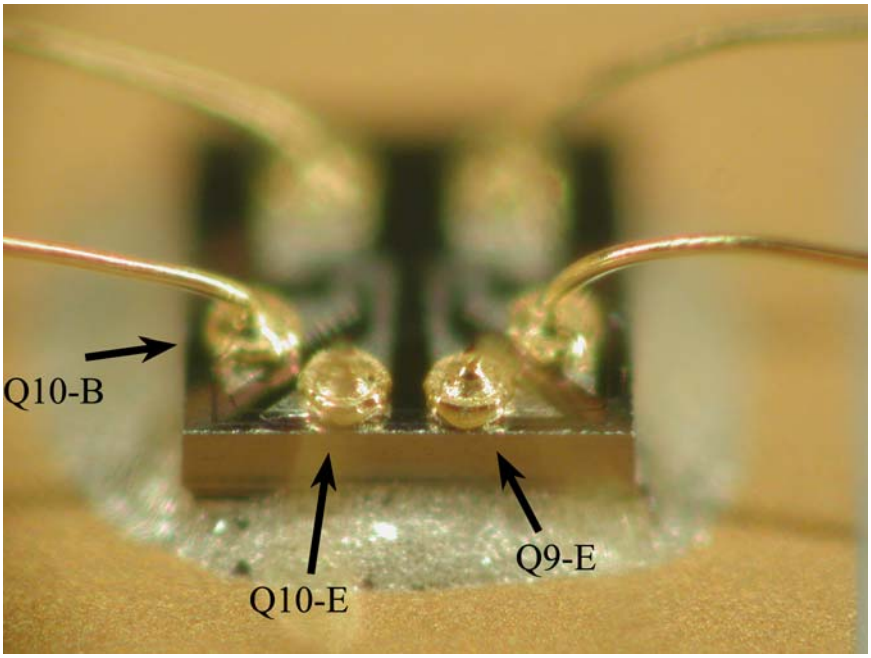

Figure 6. Angled view shows placement of ball bonds.

NASA GODDARD SPACE FLIGHT CENTER

Part Type:	Hybrid	Part No:	A111F
Manufacturer:	Amptek	Date Code:	0048

Appended Images:

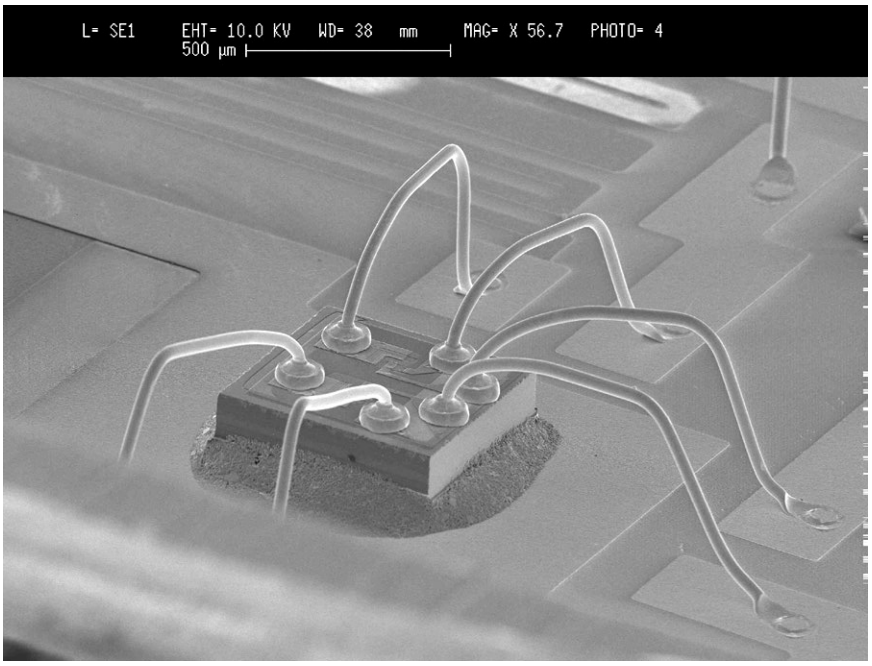

Figure 7. Macro SEM image shows the Q9/Q10 transistor die.

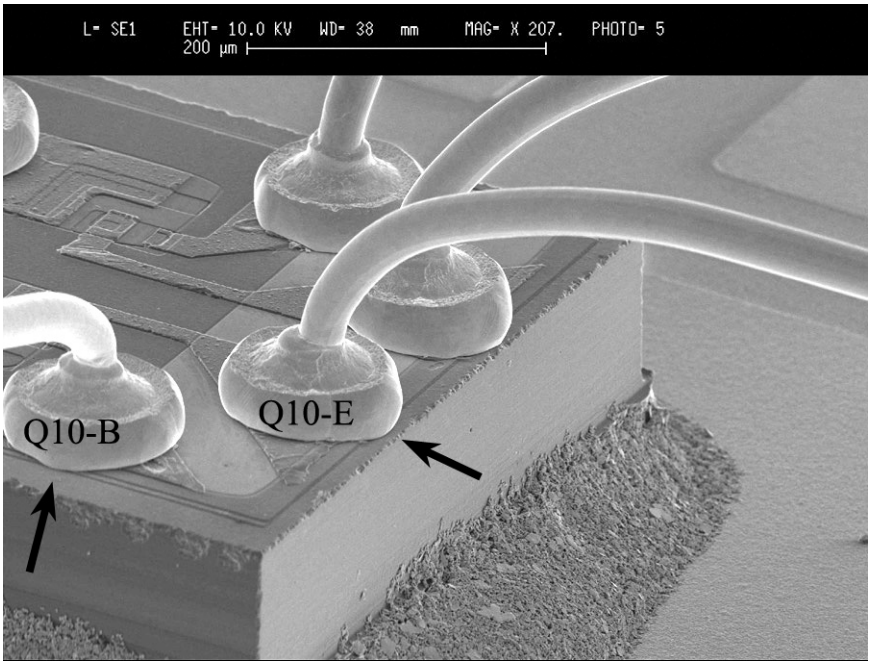

Figure 8. Close-up view shows the relatively large diameter ball bonds touching the unpassivated die edge of the die.

Part Type: Hybrid Part No: A111F
Manufacturer: Amptek Date Code: 0048

Appended Images:

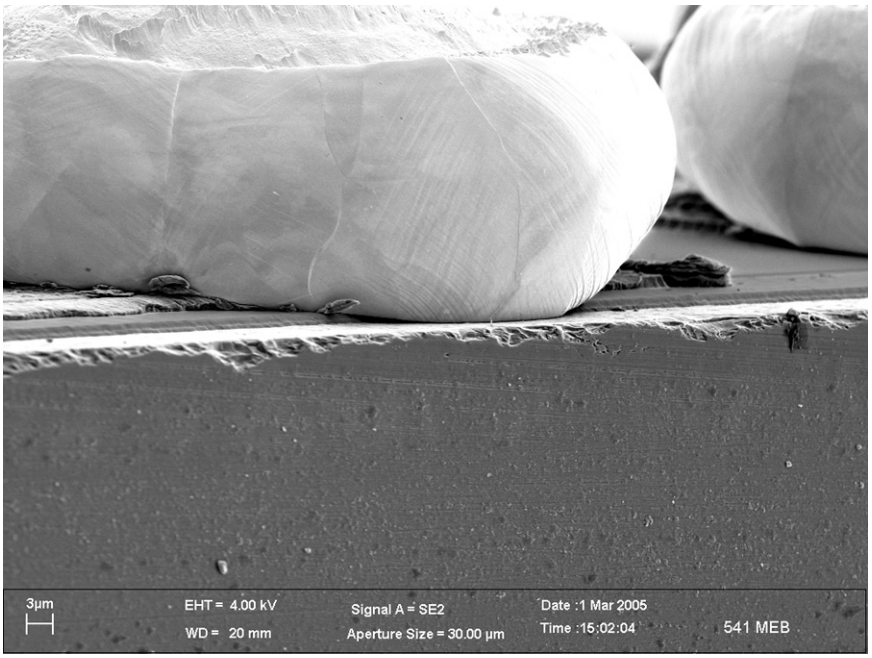

Figure 9. High magnification, high tilt, SEM view of the Q10-E ball bond touching the unpassivated die edge.

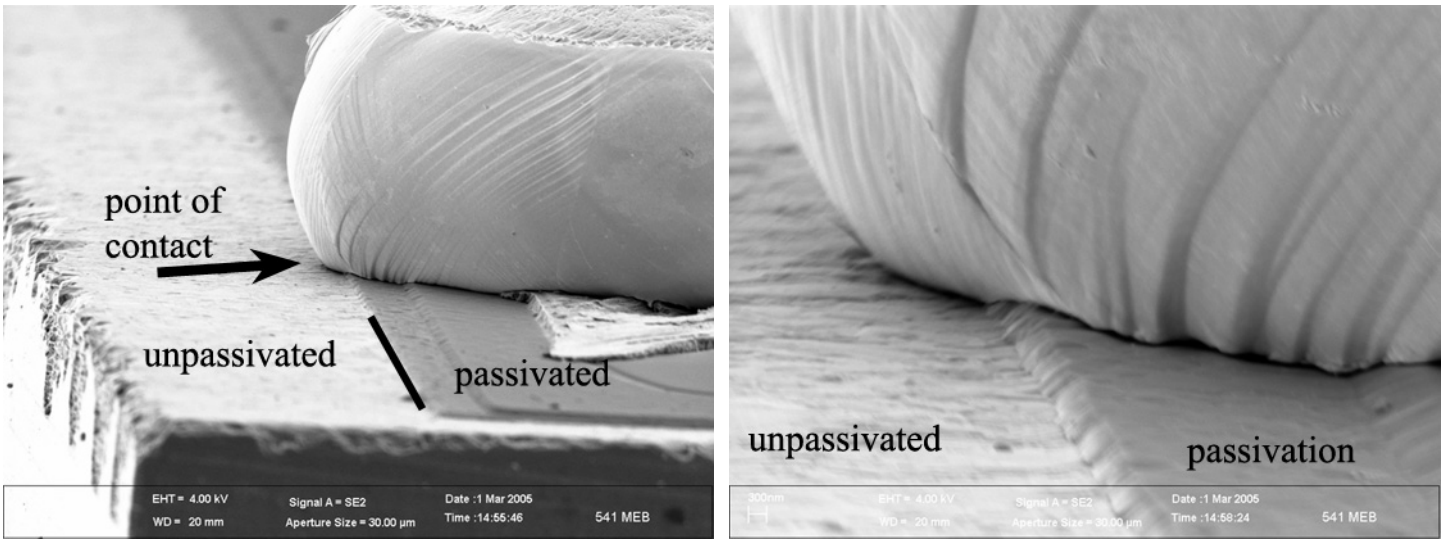

Figure 10. Similar views of Q10-B ball bond. A very small point of contact is suggested.

NASA GODDARD SPACE FLIGHT CENTER

Part Type:	Hybrid	Part No:	A111F
Manufacturer:	Amptek	Date Code:	0048

Appended Images:

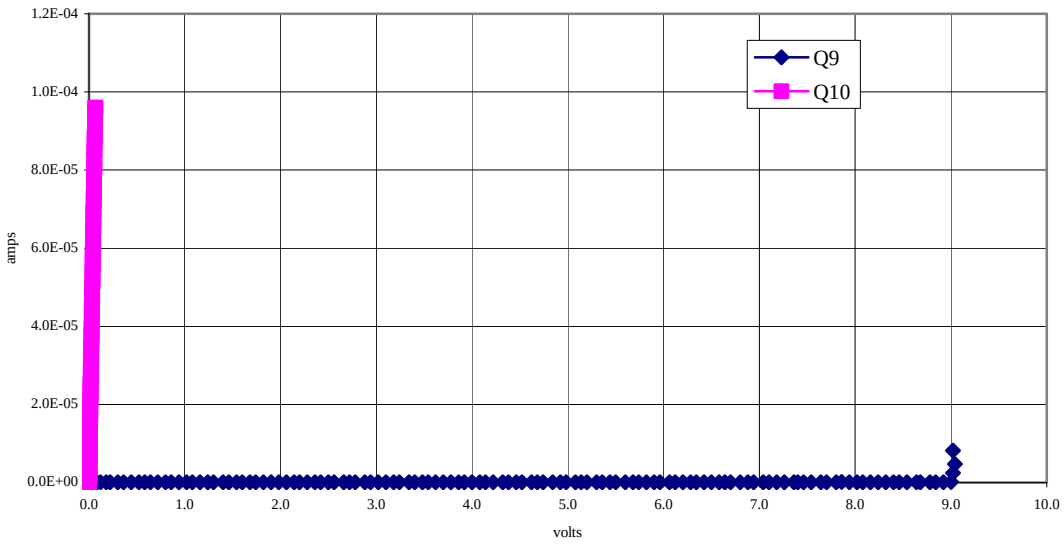

Figure 11. Emitter-base diode reverse bias [V(br)EBO] characteristic for Q9 and Q10 *prior* to removing the Q10-B ball bond from the die. The slope of the Q10 line is 687-ohms.

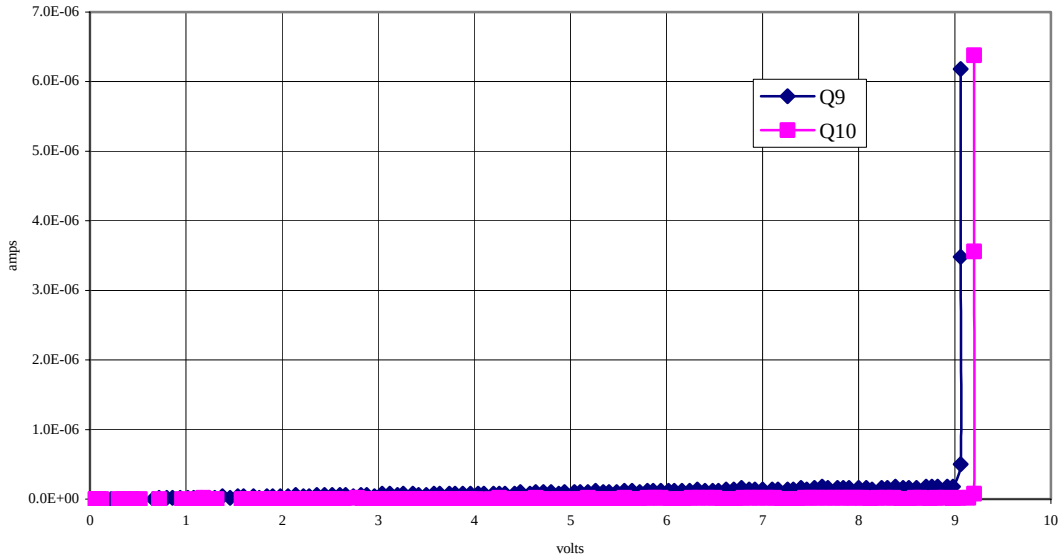

Figure 12. Emitter-base diode reverse bias characteristics *after* removing the die from the package and the Q10-B ball bond from the die.

Part Type: Hybrid Part No: A111F
Manufacturer: Amptek Date Code: 0048

Appended Images:

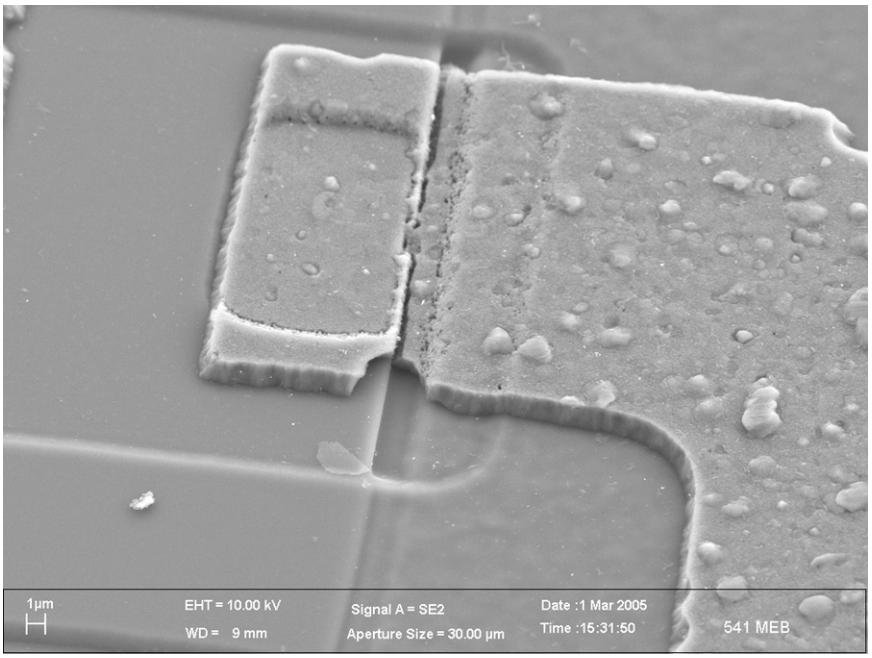

Figure 13. SEM micrograph image shows unacceptable metallization step coverage on the Q9/Q10 transistor.

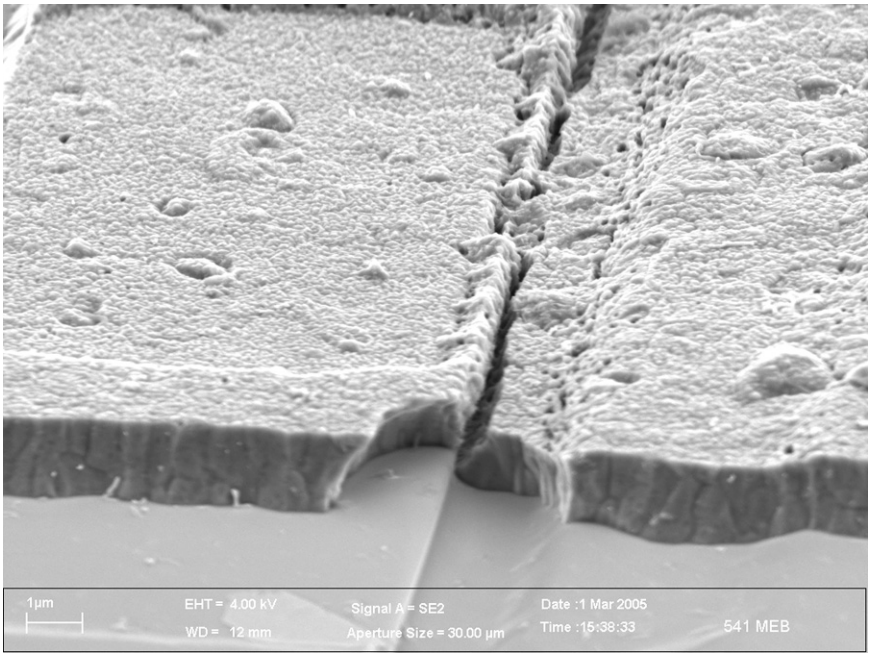

Figure 14. Close-up view of the step coverage shown above.

GODDARD SPACE FLIGHT CENTER

Evaluation and Failure Analysis Report

Charge Sensitive Pre-Amp & Discriminator Hybrid
Mfr.: Amptek, Inc.
P/N: A111F
DC: 0048
SN: 232, 233, 242, 243, 244, 246, 247

Investigator
A. Teverovsky (562)
C. Greenwell (562)

Project
STEREO
System
IMPACT-SWEA/STE-DF1
Requester
A. Reyes (562)
Report Date
09/15/2005

Background

Three failures of Amptek A111F hybrid microcircuits have occurred during testing of STEREO/IMPACT-SWEA/STE-DF1 hardware. Failure analysis of these parts (see reports Q50006FA, Q50148FA, and Q50175FA) revealed insufficient quality control of components used for assembly of the hybrids and poor workmanship, which was related to the observed failures.

The two major areas of reliability concern were wire bonding on one of the transistor dice and metallization step coverage, coincidentally, on the same transistor dice. The wire bonding was performed to a relatively small aluminum contact pad, so that a large portion of the gold ball was outside the pad area and apparently shorted the unpassivated die edge. This type of defects was responsible for one of the observed failures (see report Q50006FA) and might be also related to another failure (see report Q50175FA). Poor metallization step coverage has a risk of causing open circuit failures due to either electromigration, when voiding is formed with time as a result of high current density in the step area, or breaks in the metal when metallization is cracking as a result of mechanical stresses developed during temperature cycling.

To evaluate reliability risks, an FRB decision recommended additional testing of the parts, which would accelerate possible failures related to the observed defects. Both failure modes, a short due to wire bond shorting to the die edge and open circuit due to cracking in the metallization step coverage are expected to develop under temperature cycling. For this reason, seven residual devices from the flight lot, DC0048, which is currently installed on the hardware, were submitted to the GSFC Parts Analysis Laboratory for temperature cycle testing and analysis of possible failures.

Part Description

The A111F is a hybrid charge sensitive preamplifier, discriminator, and pulse shaper developed especially for instrumentation employing microchannel plates (MCP), channel electron multipliers (CEM), photomultipliers, proportional counters and other low capacitance charge producing detectors in the pulse counting mode. The A111 was designed specifically for NASA deep space probes, but has found other uses in space, laboratory and commercial applications.

The device is built using standard hybrid microelectronic construction. A single-sided ceramic substrate with laser-trimmed thick film resistors has several diodes, transistors, capacitors and a surface mount resistor, mounted to it with conductive and non-conductive epoxies. The discrete devices and lead frame are interconnected with 0.8, 1.0 and 1.25-mil gold bond wires. The device is provided in a hermetic, 6-pin, single in-line, metal package.

Test plan

The evaluation plan consisted of initial electrical measurements followed by unbiased temperature cycling (TC) between -65°C and +150°C with 10-minute dwell and transfer times. Interim electrical measurements were repeated at room temperature after 10, 100, 310, and 500 cycles.

Test results

Electrical measurements (see Figure 1) did not reveal significant variations of the parameters of the parts during temperature cycling. All parts passed measurements after 10 and 100 TC; however, one part, SN 244, failed functional testing with no output after 310 cycles. However, the device did provided an analog monitor output and its power supply current was within the specification limits.

The remaining six devices, SNs 232, 233, 242, 243, 246 and 247, passed electrical measurements following 310 and 500 temperature cycles.

Results of Failure Analysis

Functional testing, which was repeated several times through this failure analysis, confirmed the failure showing no signal at the output pin 6. However, the analog monitor output was present and the power supply current was nominal.

External and radiographic inspections of SN 244 revealed no anomalies. The device passed hermeticity and PIND testing. Pin to pin curve tracer testing revealed no anomaly. An overall internal view of the part is shown in Figure 2.

Initially, transistors Q5 and Q6 were suspected of causing the failure due to a photolithography defect revealed during internal examination, see Figure 3. This defect appeared to bridge the collector tub to the die substrate through an isolation diffusion, which is rejectable per MIL-STD-750, Method 2072 inspection criteria.

The backside of Q5 die is connected to V+ terminal though a 100-ohm resistor. Transistors Q5 and Q6 were isolated from the circuit by removing the interconnect bond wires. Probing the individual transistors revealed no anomalies. The characteristics of each pin combination, including each pin to the substrate, were nearly identical, suggesting that this defect was not involved in the device failure.

Internal examination revealed a misplacement of the ball bond at Q9, which was apparently sufficient to cause the ball to contact the unpassivated die edge (see Figure 4). However, electrical probing revealed no anomaly with Q9 but instead showed an open circuit at the base of Q10 (see Figure 5). Close inspection of Q10 in the SEM showed that the base metallization at an abrupt oxide step was cracked and discontinuous. The same step on Q9 looked very bad as well; however, electrical probing showed no discontinuity at this step. Figures 6 through 9 show these findings.

Discussion

As it was suspected initially, this failure analysis confirmed that the root cause of failure is related to poor metallization step coverage and that mechanical stresses during temperature cycling might result in cracking and failure due to low-cycling fatigue damage to metallization. The acceleration factor of fatigue failures can be estimated using a simplified version of Coffin-Manson model:

$$A = \left(\frac{\Delta T}{\Delta T_o} \right)^q ,$$

where q is the Coffin-Manson exponent; ΔT is the temperature interval during accelerated testing, and ΔT_o is the temperature interval during operation of the part.

The value of the exponent q is determined empirically for different groups of materials. Typically, for ductile materials, q varies from 1 to 3, but for brittle materials it can be as high as 6 to 8. For materials commonly used in microcircuits q is assumed to be between 3 and 5. Including worst-case situations (low q values) it is reasonable to presume that in our case the exponent varies from 1 to 5.

The temperature range during ground phase testing of the SWEA instrument is from -40 to +40 ^{o}C. Once the satellite is on orbit the thermal environment is rather stable and maximum expected range of temperatures is from -22.9 to +16.2 ^{o}C. Accelerating factors were calculated for both temperature conditions and the number of cycles, which is equivalent to 100 cycles between -65 and +150 ^{o}C is shown in Table 1.

Table 1. Number of cycles equivalent to 100 TC -65 to +150 ^{o}C

Temp. range	q = 1	q = 3	q = 5
-40 to +40 ^{o}C	2.7E+02	1.9E+03	1.4E+04
-22.9 to +16.2	5.5E+02	1.7E+04	5.0E+05

Based on our data, the part can withstand 100 accelerated cycles without failures. Assuming that on the orbit, the instrument will experience one cycle per day, the estimated time-to-first-failure varies from ~1.5 year at q = 1 to 45.5 years at q = 3 and even to 1380 years at q = 5.

Conclusion

One out of seven A111F hybrid microcircuits, SN244, failed after 310 temperature cycles between -65 and +150 ^{o}C. All parts passed testing after 100 TC and no additional failures occurred after 500 TC. All electrical characteristics of the parts, except for SN244, remained stable through these testing.

The failure was due to open circuit in the base metallization of transistor Q10. It appears that the thermal cycling induced enough plastic deformation in the metallization that eventually an open circuit developed at a relatively steep oxide step. Based on examination of another transistor on this die and findings of prior failure analyses, it is suspected that this die, and most likely the whole lot of these transistors, had poor step coverage metallization initially.

A serious photolithography-related defect was observed on another transistor within this hybrid. This defect, while rejectable, did not appear to play a part in the device failure.

A poor placement of the wire bond, which created a risk of shorting between the ball and the edge of the die was also observed in SN244. Similar unacceptable workmanship has been documented in other FA reports on A111F devices, and was attributed to a failure of at least one device.

Estimations of the time-to-first-failure based on accelerated temperature cycling of 7 hybrids have shown that the part likely can withstand more than 1.5 years of operation with daily cycling from -22.9 to +16.2 ^{o}C. However, additional testing should be done to get more accurate reliability predictions for the hybrids with excessive history of problems.

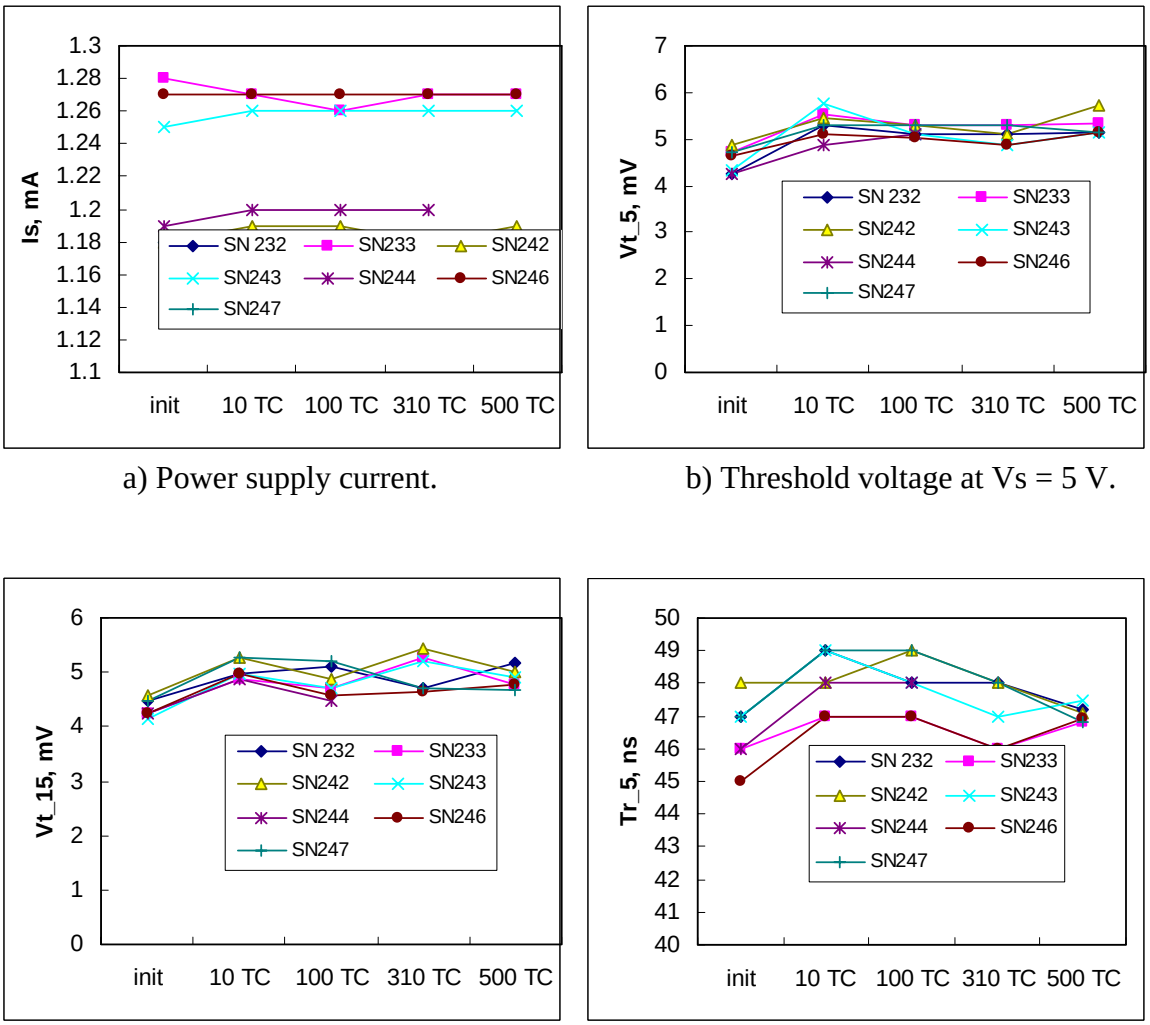

a) Power supply current.

b) Threshold voltage at Vs = 5 V.

c) Threshold voltage at Vs = 15 V.

d) Output rise time.

Figure 1. Variation of electrical characteristics during temperature cycling.

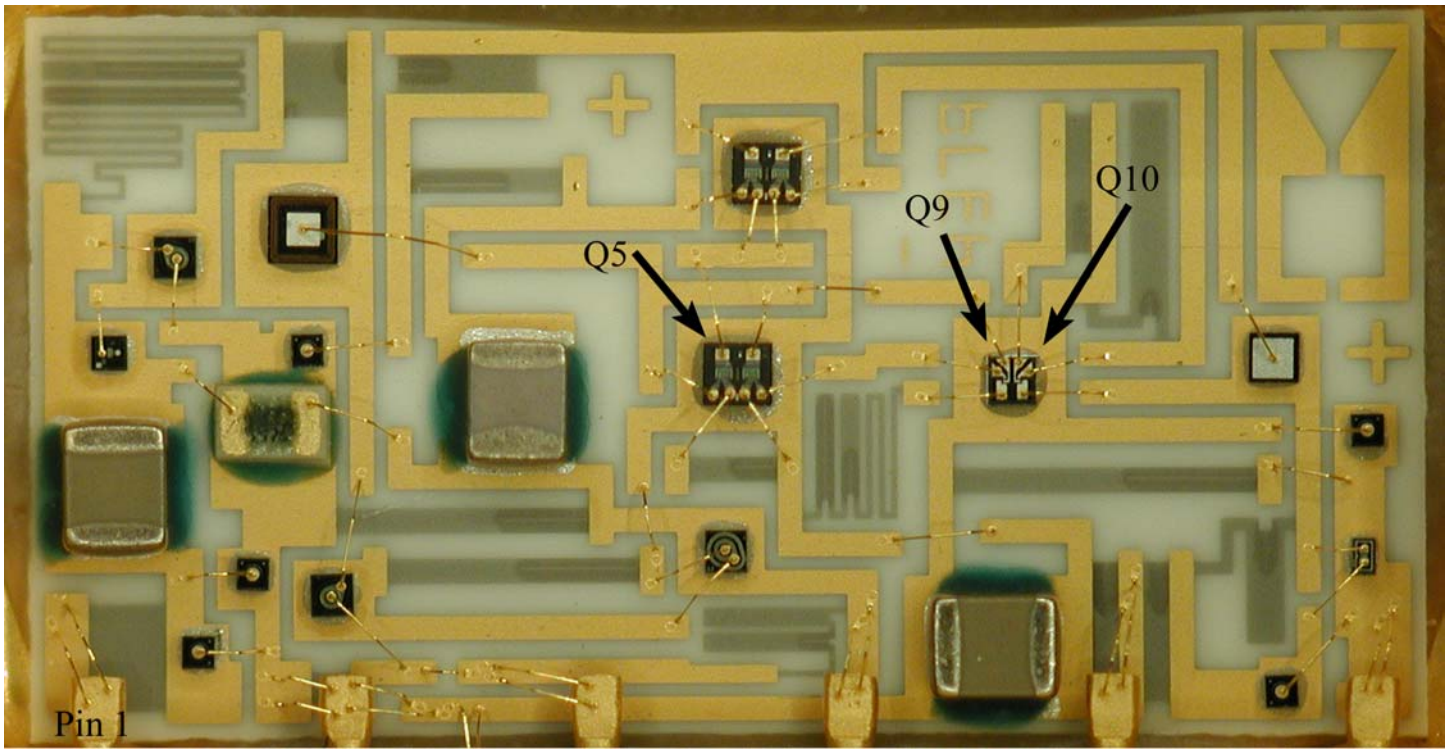

Figure 2. Internal view of the A111F SN 244 device.

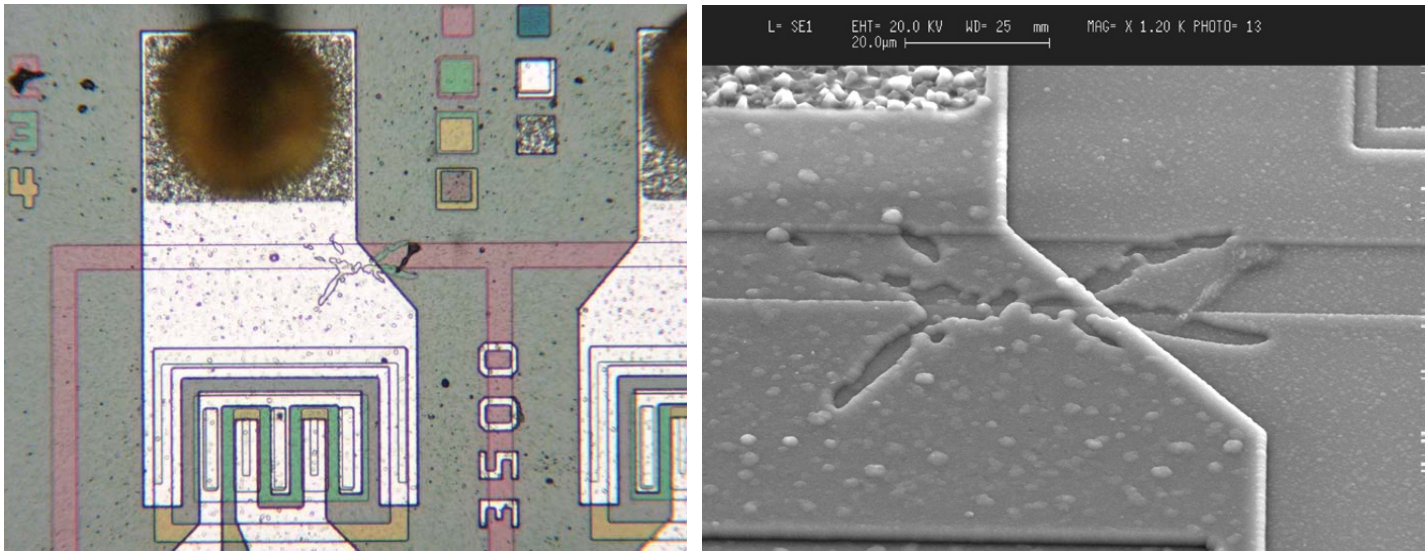

Figure 3. Optical and SEM images show defect on Q5. Probing revealed no anomaly at this device; however, this defect is rejectable per MIL-STD-750 inspection criteria.

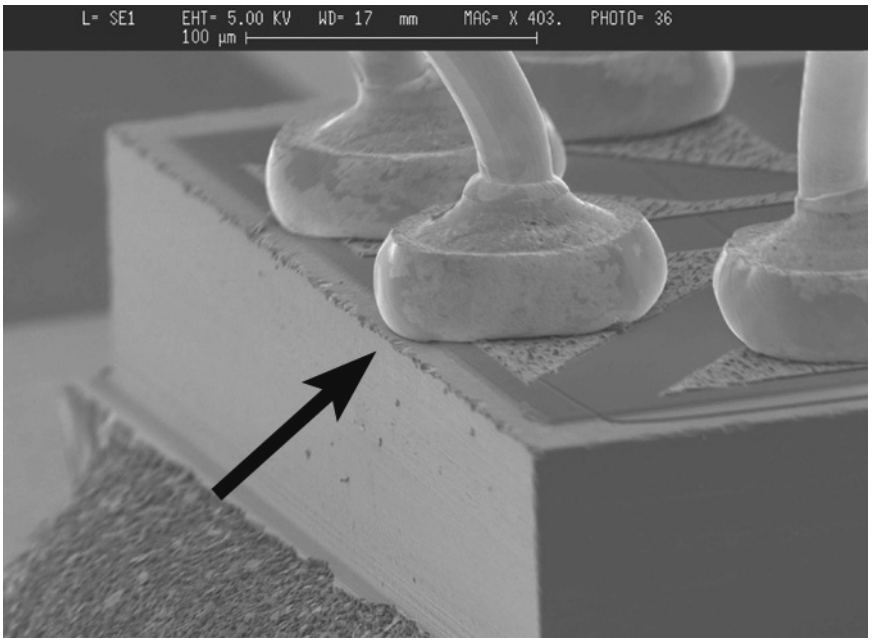

Figure 4. SEM image shows poorly placed wire bond at Q9-base.

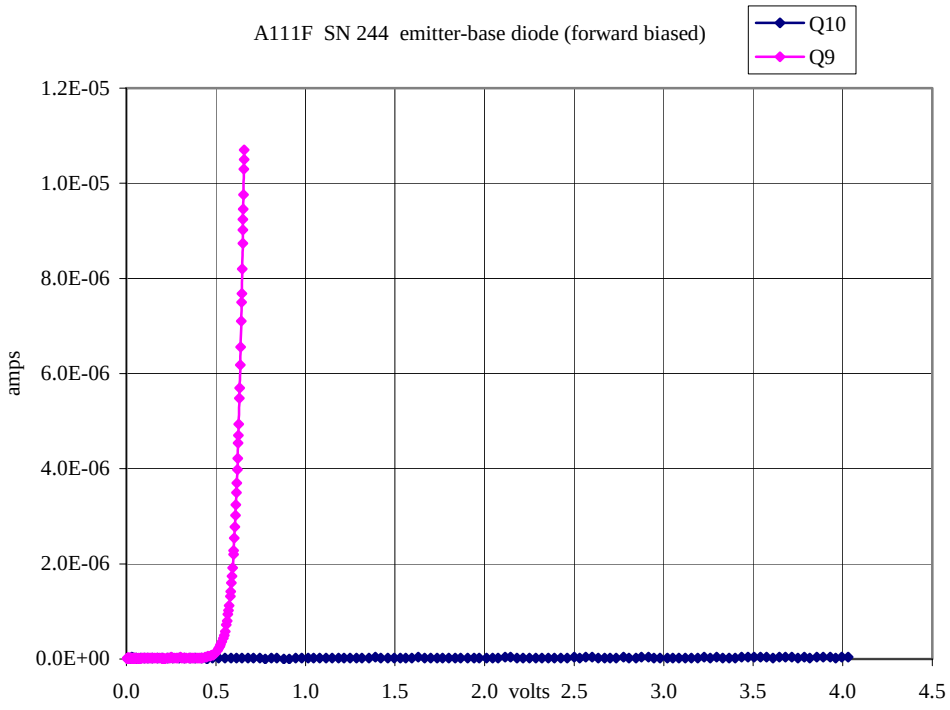

Figure 5. Curve tracer data shows normal emitter-base diode (forward bias) for Q9, while Q10 shows an open circuit. Collector-emitter characteristics were OK for both transistors.

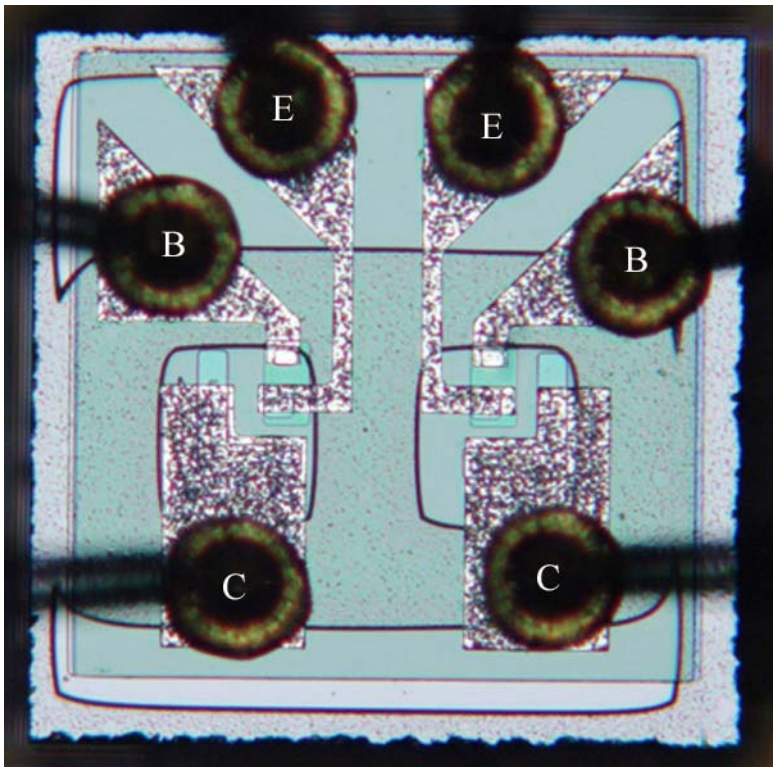

Figure 6. Optical images of Q9/Q10 die. Q9 is on the left, Q10 on the right.

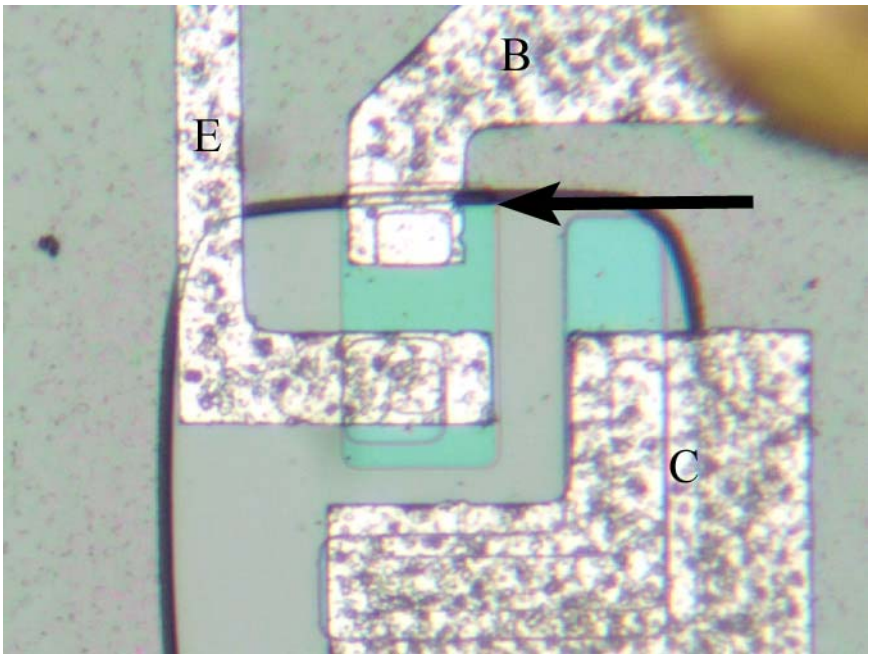

Figure 7. Close-up of Q10 with arrow showing location of open base metallization.

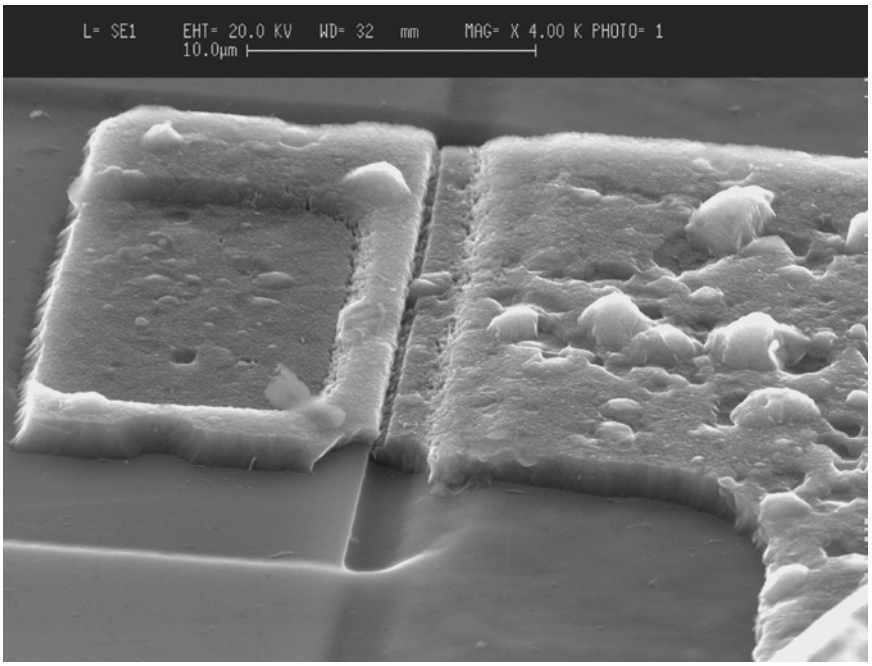

Figure 8. SEM image shows open Q10 base metallization at oxide step. (Same step as shown in Figure 7).

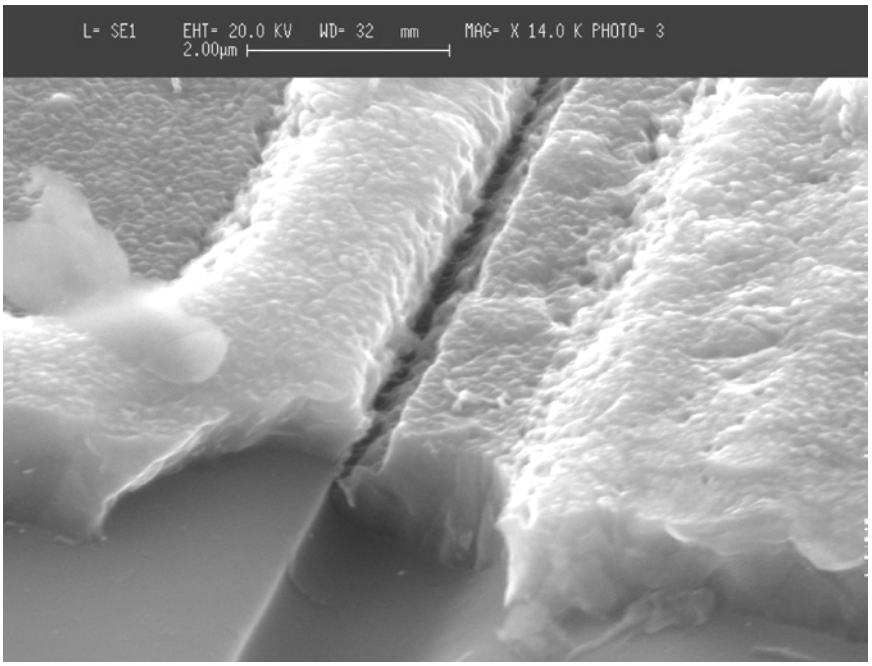

Figure 9. Close-up SEM image shows detail of separated Q10 base metal at the oxide step.